EPJ Web of Conferences **66**, 03036 (2014)
DOI: 10.1051/epjconf/ 2014 6603036

Elastic scattering of the halo nucleus ^{11}Be on ^{64}Zn

M.Hemalatha[1,a]

[1] *UM-DAE Centre for Excellence in Basic Sciences, Mumbai 400098, India*

Abstract. Elastic scattering cross sections for the halo nucleus ^{11}Be incident on ^{64}Zn in vicinity of Coulomb barrier are calculated using the microscopic double folding model. The parametrized densities taking into account for the halo part are folded with the effective nucleon-nucleon interaction (M3Y) to yield the microscopic double folded potential. The dynamic polarization potential has been computed using the dipole strength distribution from the cluster model and from experiments. The calculated differential cross section with the inclusion of the imaginary part of the dynamic polarization potential to the double folded potential show a suppression in the Coulomb-nuclear interference region.

1 Introduction

Elastic scattering, though a well-understood phenomenon, has recently attracted considerable interest due to its role in the understanding of the properties of halo nuclei, such as ^{11}Li and ^{11}Be. Halo nuclei have unusual features: small binding energy and a large interaction cross section [1]. It is expected that elastic scattering angular distributions for halo nuclei would exhibit anomalous behaviour. This effect, due to the weakly bound nature of halo projectiles, makes the coupling to the continuum relevant and can be taken into account by introducing dynamic polarization potential in the optical potential. Recently, a significant reduction in elastic scattering cross section has been experimentally observed for ^{11}Be scattering off a ^{64}Zn target at a centre-of-mass (c.m.) energy, $E_{c.m.}$ = 24.5 MeV [3]. In this article, elastic scattering cross section for ^{11}Be + ^{64}Zn at $E_{c.m.}$ = 24.5 MeV has been investigated in the framework of the double folding model with and without dynamic polarization potential. The calculation for obtaining the double-folded potential, dipole strength distribution, dynamic polarization potential and cross sections are presented in the next sections.

2 Methodology

2.1 Double folding potential

The double folding (DF) model approach [4, 5] involves determining the optical model potential by folding a complex nucleon-nucleon effective interaction with the nuclear density distributions of both projectile and target. Here, the M3Y interaction [6] modified for single-nucleon exchange [4] is used. The nuclear matter density of a one-neutron halo nucleus, ^{11}Be, is considered to be composed of

[a] e-mail: hema@cbs.ac.in

density of ^{10}Be core and density of one neutron outside the core. The density of the ^{10}Be core is considered to have a Fermi form [7] with root mean square (rms) matter radius, $< r_m^2 >_{rms}^{1/2}$ of 2.30 fm [8]. The density of the one-neutron halo is ascribed a Gaussian form [9] and the parameters of this density are adjusted to obtain $< r_m^2 >_{rms}^{1/2}$ of 2.73 fm [8] for ^{11}Be. The real part of the microscopic potential for elastic scattering of ^{11}Be + ^{64}Zn at $E_{c.m.}$ = 24.5 MeV is obtained in the DF model. In the present analysis, the imaginary part is assumed to be the same as the real part of the DF potential.

2.2 Dynamic polarization potential

The main component in the calculation of the dynamic polarization potential (DPP) is the dipole strength, $B(E1)$, distribution function. The $B(E1)$ distribution has been calculated in the simple Cluster Model (CM) [10, 11]. In CM, the nucleus is considered to break up into two fragements and is characterized by threshold energy. The dipole strength distribution as a function of excitation energy above the breakup threshold for ^{11}Be calculated using the cluster model is shown in Fig. 1 along with the corresponding experimentally measured values [12] [13]. From the figure, it can be seen that the peak value from the CM calculation is significantly higher when compared to data. It should be noted that that there is a $1/2^-$ bound first excited state in ^{11}Be at 0.32 MeV with a large $B(E1; 1/2^+ \rightarrow 1/2^-)$ = 0.115e^2 fm^2. However, coupling to this channel does not produce a significant absorptive contribution to the imaginary part of the DPP [3, 14]. Hence this state has not been included in the calculated $B(E1)$.

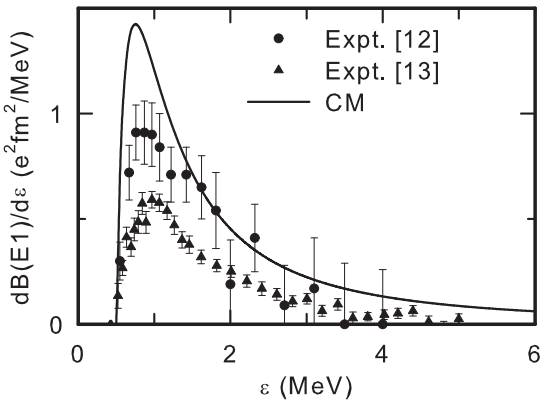

Figure 1. Calculated dipole strength distribution as a function of the excitation energy above the breakup threshold along with the experimental values for ^{11}Be [12] [13].

The DPP due to Coulomb excitation of a dipole state with excitation energy can be derived in a semi-classical way and it depends explicitly on the $B(E1)$ distribution [2, 15]. Using the $B(E1)$ distribution calculated from the CM as described above and from experimental values for ^{11}Be [12, 13], the complex DPP are determined for ^{11}Be + ^{64}Zn at $E_{c.m.}$ = 24.5 MeV and are shown in Fig. 2. The real (V_{DPP}) and imaginary (W_{DPP}) parts of DPP calculated using $B(E1)$ distribution from Ref. [12], Ref. [13] and CM are designated by D1, D2 and D3. As seen from figure, the real part of the DPP is stronger than the corresponding imaginary part. Further, it is seen that the real and imaginary parts of D3 are relatively higher than that for D2 and D1.

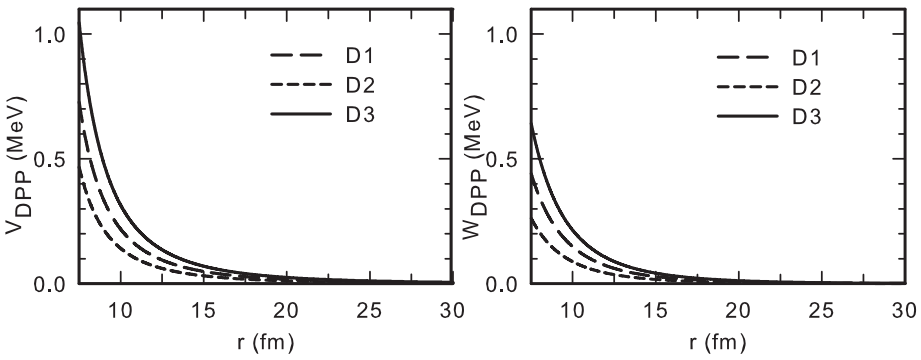

Figure 2. Real and imaginary parts of the calculated dynamic polarization potential for ^{11}Be + ^{64}Zn at $E_{c.m.}$ = 24.5 MeV.

3 Results

The real (V_{DPP}) and imaginary (W_{DPP}) parts of the calculated dynamic polarization potential calculated are added to the corresponding double folded potential (V_{DF} and W_{DF}) to give the total potential which is expressed as,

$$U(r) = \lambda_V[V_{DF}(r) + V_{DPP}(r)] + i\lambda_W[W_{DF}(r) + W_{DPP}(r)] \quad (1)$$

where λ_V and λ_W are the renormalization parameters for real and imaginary parts of the total potential. A search on λ_V and λ_W was carried out to give the best fit to the differential cross section data. The present analysis was carried out with the imaginary part of the DPP included to the DF potential as the real part has only a smaller influence on the elastic scattering cross section. The real and imaginary parts of the DF potential with and without including imaginary DPP calculated using different $B(E1)$ distributions were used to obtain differential and total reaction (σ_R) cross sections. A renormalization for real (λ_V = 0.2) and imaginary (λ_W = 1.0) parts of DF potential with imaginary DPP included for ^{11}Be + ^{64}Zn at $E_{c.m.}$ = 24.5 MeV was required to fit the data.

The angular distribution of ^{11}Be + ^{64}Zn elastic scattering (relative to Rutherford scattering cross section) at $E_{c.m.}$ = 24.5 MeV calculated with and without the inclusion of imaginary DPP are presented in Fig. 3 and are compared with the experiment [3]. The DF calculations agree with the data at forward and backward angles but do not reproduce the observed suppression in the Coulomb-nuclear interference (CNI) region. However, all the DF calculations with imaginary part of DPP (D1, D2 and D3) included show a significant suppression in the elastic scattering cross section in the CNI region and also agrees well with data at forward and backward angles. Thus, it is evident that the DPP effects cannot be ignored while determining the cross section of halo nuclei.

4 Summary

To summarize, the microscopic double folded potential and cross section for ^{11}Be + ^{64}Zn elastic scattering in the vicinity of Coulomb barrier are calculated within the framework of the double folding model. The real and imaginary parts of the DF potential are constructed by folding the M3Y effective nucleon-nucleon interaction with the nuclear matter densities of target and projectile. To take into account the dynamic coupling to the channels, the dynamic polarization potentials are calculated using

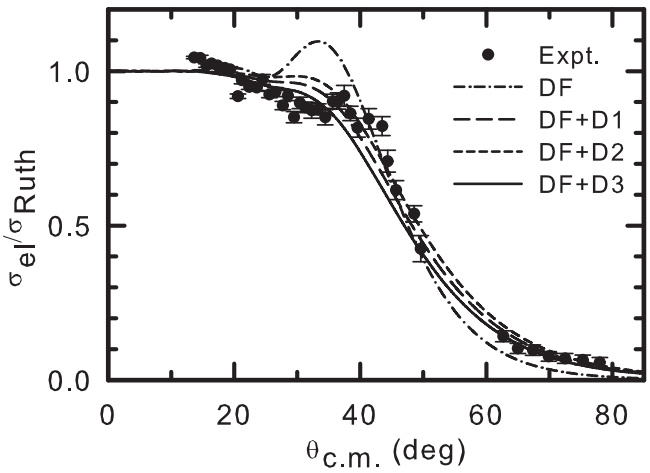

Figure 3. Calculated elastic scattering angular distribution (relative to Rutherford scattering cross section) for ^{9,10,11}Be + ^{64}Zn at $E_{c.m.}$ = 24.5 MeV.

the dipole strength distributions obtained by cluster model and from experiments. The differential and reaction cross sections are computed by using the real and the imaginary parts of the DF with and without incorporating imaginary DPP calculated from the different choices of dipole strength distributions. The DF calculations with DPP included, show a significant suppression of differential cross section for ^{11}Be + ^{64}Zn. This indicates that DPP effects due to $B(E1)$ distribution are crucial in explaining the elastic scattering cross section of halo nuclei at incident energies in the vicinity of Coulomb barrier.

References

[1] I. Tanihata *et al*., Phys. Rev. Lett. **55**, 2676 (1985).
[2] M.V. Andres *et al*., Phys. Rev. Lett. **82**, 1387 (1999).
[3] A. Di Pietro *et al*., Phys. Rev. Lett. **105**, 022701 (2010).
[4] G.R. Satchler and W.G. Love, Phys. Rep. **55**, 183 (1979).
[5] J. Cook, Comput. Phys. Commun. **25**, 125 (1982).
[6] G.F. Bertsch *et al*., Nucl. Phys. A**284**, 399 (1977).
[7] R.E. Warner *et al*., Phys. Rev. C **54**, 1700 (1996).
[8] I. Tanihata *et al*., Phys. Lett. B**206**, 592 (1988).
[9] A.K. Chaudhuri, Phys. Rev. C **49**, 1603 (1994).
[10] C.A. Bertulani *et al*., Nucl. Phys. A**526**, 751 (1991).
[11] Y. Alhassid, *et al*., Phys. Rev. Lett. **49**, 1482 (1982).
[12] T. Nakamura *et al*., Phys. Lett. B**331**, 296 (1994).
[13] R. Palit *et al*., Phys. Rev. C **68**, 034318 (2003).
[14] N. Keeley *et al*., Phys. Rev. C **82**, 034606 (2010).
[15] M.V. Andres *et al*., Computer code POLPOT, unpublished (2006).